Forest Ecology and Management 618 (2026) 124040

Contents lists available at ScienceDirect

Forest Ecology and Management

journal homepage: www.elsevier.com/locate/foreco

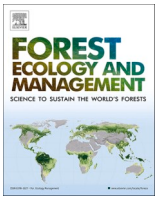

National vulnerability models for wind and snow damage based on airborne laser scanning and National Forest Inventory data

Inka Bohlin [a,*], Emanuele Papucci [a], Victor Manabe [b], Sven Adler [a], Olivia Fors [a], Bertil Westerlund [a], Susanne Suvanto [c]

[a] Swedish University of Agricultural Sciences (SLU), Department of Forest Resource Management, Skogmarksgränd 17, Umeå 907 36, Sweden
[b] Swedish University of Agricultural Sciences (SLU), Department of Crop Production Ecology, Skogmarksgränd 17, Umeå 907 36, Sweden
[c] Natural Resources Institute Finland (Luke), Latokartanonkaari 9, Helsinki 00790, Finland

ARTICLE INFO

Keywords:
ALS
NFI
Damage probability
Wind damage
Snow damage
Sweden

ABSTRACT

In this study we created national vulnerability models for wind and snow damage based on a combination of remote sensing and Swedish National Forest Inventory (NFI) data and compared the performance of airborne laser scanning (ALS) driven versus field-measured information in the modeling of damage vulnerability. The empirical training data consisted of circa 42,000 field plots, containing information about recent wind and snow damage, monitored between 2010 and 2022 in the Swedish NFI. Occurrence of damage was predicted using variables calculated from national ALS data (2009–2023), other mapped products including forest attributes, soil and terrain related data and spatial variables on stand neighborhood, and weather data. In contrast to earlier large-scale damage models, we used direct ALS metrics to fully exploit ALS-derived forest structural information. Logistic regression was used for modeling, and separate models were created for southern and northern Sweden to consider the geographical differences in forest structure and climate conditions. Field data-based models performed slightly better than remote sensing (RS) -based models, resulting in an AUC of 0.8 for northern and 0.73 for southern Sweden. Corresponding results for RS-based models were 0.77 and 0.69. Best models included both forest structural variables (ALS or field-based), tree species, terrain, and weather information. We successfully demonstrated the combination of ALS and NFI data to map forest vulnerability to wind and snow damage, enabling evaluation of damage vulnerability from stand to national level. By locating areas with high damage vulnerability, forest owners can more easily adapt forest management to increasing climate impacts.

1. Introduction

Wind and snow are the most important abiotic causes of forest damage in Northern Europe (Skogsdata, 2007; Korhonen et al., 2021). In Sweden, 2.3% of productive forest land has been affected by wind and snow damage over the last five years (Skogsdata, 2025). While these damages in boreal forests are part of the natural disturbance dynamics of the ecosystem, they also have considerable negative consequences. Damaged trees lead to direct losses in wood value, and falling and breaking trees may cause substantial disruption to infrastructure, such as power lines, roads, and railway networks (Groenemeijer et al., 2015; Räisänen et al., 2023; Gardiner et al., 2024). Furthermore, abiotic forest damage may lead to subsequent infestations by insects or infections by fungi (Nykänen et al., 1997; Komonen et al., 2011), and in large-scale events, salvage logging of the damaged wood can impact wood markets and prices (Asada et al., 2023). To account for damage risks in forest management decisions, it is essential to quantify vulnerability to damage in different types of forests and under different site conditions. This becomes increasingly important as climate change is altering forest disturbance regimes, creating an urgent need to adapt forest management to increase the resilience of boreal forests.

The processes involved both wind and snow damage are somewhat similar with the force of wind and/or snow load exceeding the mechanical resistance of trees, leading to stem or branch breakage or uprooting (Peltola et al., 1999). The factors influencing the probability of wind and snow damage relate to specific meteorological conditions, such as wind speed and gustiness (Gardiner, 2021) or snow load in the tree crowns (Lehtonen et al., 2016). However, other factors are also crucial in understanding when and where damage occurs, including the structure and composition of the forest, recent forest management

* Corresponding author.
E-mail address: inka.bohlin@slu.se (I. Bohlin).

https://doi.org/10.1016/j.foreco.2026.124040
Received 17 April 2026; Received in revised form 16 June 2026; Accepted 18 June 2026
Available online 24 June 2026

operations, and site properties such as soil and topography (Nykänen et al., 1997; Mitchell, 2013). In the case of wind damage, vulnerability typically increases with tree height and slenderness, and several studies have found Norway spruce to be more susceptible to wind compared to Scots pine and broadleaved trees (Peltola et al., 1999; Valinger and Fridman, 2011; Suvanto et al., 2019). Typical cases of high wind risk are trees along new stand edges and recently thinned forests, where previously sheltered trees are exposed to stronger wind conditions (Peltola et al., 1999; Valinger and Fridman, 2011; Wallentin and Nilsson, 2014; Suvanto et al., 2019). Damage caused by snow is typically found in young and dense stands and it is observed to occur more often in Scots pine compared to Norway spruce stands, and more commonly in conifer stands than in broadleaved stands (Nykänen et al., 1997; Suvanto et al., 2021).

The most optimal modeling and mapping of damage vulnerability demands different approaches, where field-based models (using forest attributes) are most suitable for simulation studies (e.g., Öhman et al., 2025), while remote sensing (RS)-based models can take into account the spatial variation in forest landscapes and apply direct remote sensing variables, such as lidar or spectral metrics (Torresani et al., 2024). A range of models have been developed for quantifying wind and snow damage vulnerability, including both mechanistic models (e.g., Peltola et al., 1999; Gardiner et al., 2008; Zubkov et al., 2024) and empirical models fitted to large datasets (e.g., Valinger and Fridman, 1997, 2011; Díaz-Yáñez et al., 2019; Hart et al., 2019; Suvanto et al., 2019, 2021). Recently, forest wind and snow damage models have been combined with spatial datasets describing the factors contributing to damage vulnerability and developed into wall-to-wall maps presenting the spatial variation in damage probability at regional or national scales (Suvanto et al., 2019, 2021; Pawlik and Harrison, 2022; Costa et al., 2023; Merlin et al., 2025). These maps provide a valuable and easily interpretable estimation of damage vulnerability in individual forest stands, supporting the consideration of damage vulnerability when planning forest management operations. While mapping damage vulnerability has recently been conducted with different types of models, National Forest Inventory (NFI) damage observations provide a valuable data source for this purpose, as they systematically cover large areas with varying meteorological and site conditions, thus reducing the need to extrapolate to conditions outside the training data of the models.

National ALS campaigns in many European countries, including Sweden, provide an improved data source for detailed quantification of forest structure with continuous coverage across large areas (Maltamo et al., 2014; Nilsson et al., 2017). ALS-based forest structure information has also been shown to be useful in the quantification of forest vulnerability to wind damage. Recently, Merlin et al. (2025) mapped wind damage vulnerability in Norway with the ForestGALES model and used partly ALS-based forest resource maps as inputs. These maps are based on the modeled relationship between ALS metrics and field-measured reference data, e.g., tree height, volume, or tree species (e.g., Maltamo et al., 2014; Nilsson et al., 2017). ALS metrics have also been used directly in forest damage modeling studies. For example, Torresani et al. (2024) showed in a case-study region in Italy that ALS-derived metrics for pre-damage forest height and density were important for quantifying the vulnerability of forests to damage in a storm. Similarly, Saarinen et al. (2016) found ALS-based forest height to be useful for modeling forest predisposition to wind disturbances in a case study area in Finland. ALS data has also been utilized for deriving inputs for mechanistic wind damage models (Gopalakrishnan et al., 2020; Costa et al., 2023).

While the use of ALS data can improve the estimates of commonly used forest attributes, the ALS point cloud also contains more detailed information about the three-dimensional structure of the forest canopy (Lefsky et al., 1999; Maltamo et al., 2014). This is important for modeling abiotic forest damage, as canopy structure and tree shape impact both the sensitivity of trees to wind (Jackson et al., 2019) and the wind conditions within the forest (Boudreault et al., 2014) in more detail than what can be described by forest attributes typically considered in forest damage models, such as tree height or gap size (e.g., Suvanto et al., 2019, 2021; Pawlik and Harrison, 2022, Costa et al., 2023, Merlin et al., 2025). ALS metrics that quantify different aspects of the canopy structure have the potential to represent more complex features of the canopy structure that affect the vulnerability of a forest to damage. Furthermore, ALS can quantify canopy structure in more detail than traditional field measurements of trees. Therefore, to reach the full capacity of ALS in forest damage modeling one needs to utilize direct ALS metrics that describe the canopy structure in detail, instead of only traditionally used ALS-based forest attributes. In addition, this approach can eliminate one modeling step and its associated prediction errors. However, exploration of different ALS metrics relevant for modeling damage vulnerability and their performance compared to commonly used field-measured forest variables is still missing.

The purpose of this study is to improve the prediction of forest vulnerability for wind and snow damage by using a combination of national data sources, including ALS data, to support decision making in forest management. More specifically, we aimed to

1) identify useful ALS metrics and combinations of RS variables in modeling wind and snow damage,
2) compare the performance of ALS driven versus field-measured information in modeling wind and snow damage vulnerability, and thereby
3) create the first national vulnerability models for wind and snow damage based on a combination of ALS and NFI data in Sweden.

For these goals, we used the Swedish National Forest Inventory (NFI) together with national airborne laser scanning (ALS) data, other forest map products including forest attributes, soil and terrain related data and spatial variables on stand neighborhood, and weather data covering the whole of Sweden.

2. Material and methods

2.1. National Forest Inventory data

In the Swedish NFI, the locations of the field plots follow a regionally dedicated sampling design, where permanent plots are visited every fifth year and temporary plots only once (Fridman et al., 2014). In this study, we used both permanent and temporary plots monitored between 2010 and 2022 for model training. The center coordinates of each NFI plot are recorded with GPS according to the NFI instructions (National Forest Inventory, 2022). We used only plots that were measured after the national laser scanning campaign (first scanning started in 2009) at the same locations, to ensure that the forest structure was captured in the ALS data before any possible damage occurred. Here, only plots in productive forest land were included, since they have higher economic value for forest owners and higher vulnerability to wind and snow damage. The dataset consisted of both undivided plots (majority) and divided plots (plot is divided based on different developing stages or soil conditions inside the plot), but on divided plots, only the sub-plot covering the largest area inside the plot was included.

In the Swedish NFI, forest damage is measured at different scales (e.g., stand, sample trees, browsing inventory) (National Forest Inventory, 2022). In this study, we used the “stand-level” damage observations of wind and snow damage, which means that the presence (yes/no) and estimated time of damage to living trees is evaluated within the 20 m radius circular plot. Wind and snow damage are recorded together as a combined category, since they are part of the same damage process (Peltola et al., 1999). Separate damage agents are recorded if damage has occurred in the last five years and when the damage grade is higher than 10%. We included plots with damage occurring after the closest laser scanning time point. The time difference between the laser scanning year and the damage year (damaged plots) or inventory year

(non-damaged plots) varied between 1 and 13 years, and the same permanent plot was included only once in the dataset. In addition, all NFI plots that were harvested between the ALS data acquisition and the field data collection were excluded from the dataset.

In this study, we excluded the most severe storm events within the study period because, in very strong storm conditions, the damage is less dependent on forest structure and composition (the strength of wind dominates where the damage occurs) (e.g., Peltola et al., 1999), which could have unpredictable impacts on model development. We used severity maps by SMHI that indicated the calculated return times (years) for gusty wind speed during the storm. We removed NFI plots in the most affected counties of storms Gudrun (2005), Hilde (2013), and Ivar (2013) showing return time more than circa 20 years (SMHI, 2025), in cases where the inventory fieldwork had been carried out within five years after the storm. The five-year window was needed, as we are using NFI plots where damage could have occurred up to five years before the inventory year. In total, 5148 NFI plots (1034 damaged plots) were removed from the data in this step. After that, the total number of plots was 42,313, and stand-level wind and/or snow damage was observed in 615 of these plots (i.e., approximately 1.5% of the plots were damaged; Fig. 1).

Several forest variables were extracted to train the NFI-based models including plot related volume, basal area, mean height, species specific basal areas and volumes of Scots pine (*Pinus sylvestris*), Norway spruce (*Picea abies),* birch (*Betula* spp.), Lodgepole pine (*Pinus contorta)* and deciduous trees other than birch, stand age, site index, soil moisture, soil type, soil texture, soil depth, field layer type describing dominating surface vegetation (dwarf-shrubs, herbs, grasses), time since thinning, distance to neighboring stand or land use class (max 25 m distance from plot center) and stand height of the closest stand (max 25 m distance). Site characteristics were measured from a 10 m radius plot and tree characteristics from a 10 m (permanent plots) or 7 m (temporary plots) radius plot. The variables selected in this study have been identified as being critical for vulnerability of wind or snow damage from previous studies (e.g., Nykänen et al., 1997; Peltola et al., 1999; Valinger and Fridman, 2011; Mitchell, 2013; Suvanto et al., 2019), i.e. not all available NFI variables were tested here. From some of the variables extracted from the NFI we derived new variables: proportion and dominant tree species (pine, spruce, lodgepole, deciduous/other), reclassified site-index (0–20,20–25,25 +), soil wetness (wet/dry) and time since thinning (less/more than 10 years), and the height difference with the closest stand. The descriptive statistics of predictor variables for damaged, non-damaged, and all plots in the field-based models are presented in Table 1.

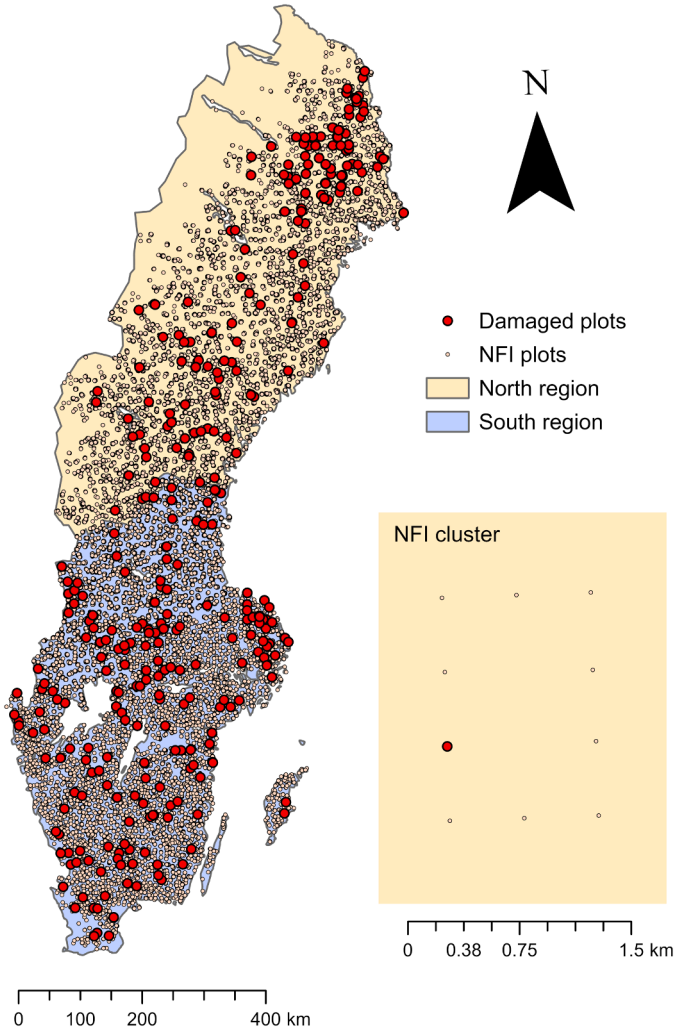

Fig. 1. Distribution of damaged and non-damaged NFI plots used in the modeling dataset across the northern and southern regions of Sweden, and an example of an NFI cluster in the North region. Each dot indicates the location of a plot or cluster, which may include multiple plots.

2.2. ALS data

The ALS data includes two national scanning campaigns (2009–2019 and 2018–2022) with point densities of 0.5 and 1–2 points/m^2 (Lantmäteriet, 2022, 2024), and data from different scanners, including both leaf-on and leaf-off conditions. We used the lidR package (Roussel et al., 2020, 2025) in R (version 4.4.0, R Core Team, 2024) to calculate height-normalized ALS metrics from all returns inside a 20 m circular plot. These metrics were used as predictor variables in our RS-based models. They describe the height and density distribution of laser returns and are commonly used for predicting forest structure. Metrics were: metrics_basic, which describes simple statistics of the height of laser returns (e.g., zmin, zmean, zkurt); metrics_percentiles, which describes the height of returns when a certain proportion of returns have accumulated (zq1, zq5, zq10, …, zq90, zq95, zq99); metrics_percabove, which describes the proportion of returns above a defined threshold (e.g., pzabovemean); metrics_dispersion, which describes the vertical structure (e.g., ziqr, CRR, VCI); metrics_canopydensity, which describes the cumulative point density (zpcum1, zpcum2, …, zpcum9); metric_Lmoments, which describes L-moments, i.e. the shape of the height distribution of returns (e.g., L1, Lskew); metrics_lad, which describes leaf area density (e.g., lad_max, lad_sum); metrics_interval, which describes the proportion of returns between specified elevation intervals (e.g., pz_below_0, pz_5_10, pz_above_30); and metrics_voxels, which describes metrics calculated in voxel space (vn, vFRcanopy, OpenGapSpace). See the full list of metrics and their description in Tompalski and Goodbody (2025).

2.3. Other map products

We employed national forest attribute maps for forest related variables (10 ×10 m grid-cells) including volume, basal area, mean diameter, and mean height metrics (Nilsson et al., 2017). These maps are derived from a combination of national ALS and NFI data. Similarly, the tree species-specific volume maps (12.5 ×12.5 m grid-cells) for pine, spruce, lodgepole, and deciduous trees are based on ALS points clouds and Sentinel−2 satellite images (SLU, 2018). The vegetation type maps (10 ×10 m grid-cells), based on Sentinel−2 images, include various land-use classes and vegetation types (Naturvårdsverket, 2023). Either the mean value of the raster cells (continuous variables) within each NFI plot or the value at the plot center (categorical variables) within each 20 m radius circle plot was extracted.

For soil and terrain related variables, we used three different datasets. The soil moisture map (2 ×2 m grid-cells) is based on ALS data, NFI

Table 1
The descriptive statistics (mean and standard deviation (in parenthesis) or proportion of the observation) of predictor variables of damaged, non-damaged and all plots in RS- and field-based (NFI) models in the North and the South regions.

Variables	Unit	Damaged	Non-damaged	ALL
RS North				
Number of plots		287	14,779	15,066
zpcum6	%	74.8 (12.4)	82.3 (12.1)	82.1 (12.1)
VolumeSpruce	m^3/ha	92.0 (88.7)	85.2 (77.4)	85.3 (77.6)
VolumeLodgepole	m^3/ha	18.6 (27.3)	6.7 (14.6)	6.9 (15.0)
Elevation	m	329.5 (129.6)	313.1 (160.6)	313.4 (160.0)
Snowdepth	cm	227.1 (72.4)	205.1 (64.5)	205.5 (64.7)
MaxWindWest	m/s	9.9 (1.2)	10.4 (1.3)	10.3 (1.3)
Leaf-on data (1)		0 = 26% 1 = 74%	0 = 18% 1 = 82%	0 = 19% 1 = 81%
RS South				
Number of plots		328	26,154	26,482
zq15	m	0.2 (1)	0.1 (0.5)	0.1 (0.5)
zq30	m	1.1 (2.3)	0.8 (2)	0.8 (2)
Pz_5.10	%	18.1 (12.6)	14.0 (11.2)	14.1 (11.2)
zpcum4	%	49.0 (17.3)	57.2 (20.6)	57.1 (20.6)
VolumeSpruce	m^3/ha	166.8 (123.1)	142.9 (107.9)	143.2 (108.1)
VolumePine	m^3/ha	131.8 (71.7)	114.0 (73)	114.2 (73)
VolumeLodgepole	m^3/ha	3.2 (10.9)	1.4 (7.1)	1.5 (7.1)
Diff_zq95_50m	m	130.1 (76.6)	120.5 (73.1)	120.6 (73.2)
Elevation1kmDiff	m	36.4 (40.7)	30.0 (31.3)	30.1 (31.4)
MaXWindNorth		8.1 (1.3)	7.9 (1.2)	7.9 (1.2)
NFI North				
Number of plots		286	15,055	15,341
Mean height	m	15.1 (4.9)	11.7 (6.4)	11.8 (6.4)
Prop. lodgepole	%	24.3 (40.5)	3.2 (16.3)	3.5 (17.3)
Prop. deciduous/other	%	7.7 (14.2)	13.1 (21.4)	13.0 (21.3)
Time since thinning > 10 years (1)		0 = 15% 1 = 85%	0 = 6% 1 = 94%	0 = 6% 1 = 94%
Snowload	kN/m^2	1.6 (0.4)	1.5 (0.4)	1.5 (0.4)
MaxWindWest	m/s	9.9 (1.2)	10.4 (1.3)	10.3 (1.3)
NFI South				
Number of plots		328	26,030	26,358
Mean height	m	18.5 (5.7)	14.5 (8.1)	14.5 (8.1)
Prop. spruce	%	48.2 (39.9)	38.8 (38)	38.9 (38)
Prop. lodgepole	%	2.4 (13.5)	0.4 (5.6)	0.4 (5.8)
Time since thinning > 10 years (1)		0 = 30% 1 = 70%	0 = 20% 1 = 80%	0 = 20% 1 = 80%
Height dif. closest stand	m	6.2 (8.8)	2.2 (5.5)	2.3 (5.6)
Elevation	m	185.0 (146.1)	168.4 (122)	168.6 (122.4)
MaxWindNorth	m/s	8.1 (1.3)	7.9 (1.2)	7.9 (1.2)

Note:
RS variables: zpcum6 = cumulative percentage of laser returns located in the lower 60% of maximum elevation, VolumeSpruce = stem volume of Norway spruce, VolumeLodgepole = stem volume of Lodgepole pine, Elevation = height above sea, Snowdepth = mean of maximum snow depth 2007–2023, MaxWindWest = mean of maximum wind speed from West 2007–2023, Leaf-on data = if laser data is collected with leaf-on or leaf-of conditions, zq15 = 15th percentiles of laser return heights, zq30 = 30th percentiles of laser return heights, Pz_5.10 = proportion of laser returns between 5 and 10 m, zpcum4 = cumulative percentage of laser returns located in the lower 40% of maximum elevation, VolumePine = Stem volume of Scots pine, Diff_zq95_50m = height difference inside a 50 m radius plot, Elevation1kmDiff = difference between mean height above sea in the plot and mean height above sea in 1 km radius circular plot, MaXWindNorth = mean of maximum wind speed from North 2007–2023.
NFI variables: Mean height = basal area weighted mean height of forest, Prop. lodgepole = proportion of Lodgepole pine from stem volume, Prop. deciduous/other = proportion of deciduous trees and other (not pine, spruce, lodgepole) from stem volume, Time since thinning > 10 years = if time since last thinning of stand is shorter or longer than 10 years, Snowload = mean of maximum snow load 2007–2023, MaxWindWest = mean of maximum wind speed from West 2007–2023, Prop. spruce = Proportion of Norway spruce from stem volume, Height dif. closest stand = height difference of forest with closest stand within 25 m, Elevation = height above sea, MaxWindNorth = mean of maximum wind speed from North 2007–2023.

data, and other map products (Ågren and Lindberg, 2020Ågren and Lindberg, 2020). The soil type (vector data) and soil depth (10 ×10 m grid-cells) maps are coarse-scale products provided by the Swedish Geological Survey (SGU, 2025a, 2025b). Finally, the digital terrain model (DTM, height above sea, 2 ×2 m grid-cells), based on laser data (Lantmäteriet, 2022), was used as a basemap for terrain variables such as mean elevation, slope, slope direction, and elevation difference within 1 km. Here, the maximum or mean value of raster cells within each plot was extracted.

Spatial variables describing height variation in the plot neighborhood were also calculated from other mapped products. They were: distance to closest clearcut (based on reported harvesting locations by Swedish Forest Agency from 2000 to 2023) (Skogsstyrelsen, 2024), distance to closest open area (based on the land use classification), and height variation inside 20 m and 50 m circular plots based on an existing raster derived from the point cloud metric zq95 (95th percentile of the height of the laser points i.e. canopy height) with 10x10m pixel size. A detailed list of variables based on RS data and other map products can be found in Appendix A. The descriptive statistics of predictor variables of damaged, non-damaged and all plots in RS-based models are presented in Table 1.

2.4. Weather data

The weather data from the Swedish meteorological institute (smhi.se) included daily mean values of temperature, wind speed and wind direction, snow depth and snow load between 2007 and 2023 (SMHI, 2023). These data are predicted for the whole country on a raster with a 11 × 11 km grid cells within the time range 2007–2014, and 2.5 × 2.5 km grid cells within the time range 2015–2023, covering the whole of Sweden. From the rasterized weather data, pixel values from the center of the NFI plots were extracted. Different predictor variables, identified to be useful for predicting damage vulnerability, were calculated from the weather dataset including mean number of days above 0 °C, mean of maximum wind speed (m/s), mean of maximum wind speed from different directions (e.g., north, west), most common wind direction, mode of max wind direction, and mean of maximum wind speed from opposite to mode of wind directions, mean of max wind speed to upslope direction, and mean of maximum snow depth (cm) and snow load (kN/m^2).

2.5. Statistical modeling and prediction to test areas

Field-based models were first developed using predictor variables from NFI data (see 2.1), weather data (2.4) and elevation (height above sea), a total of 53 variables were tested. RS-based models were developed using predictor variables from ALS data (2.2), other mapped products (2.3) and weather data (2.4), and a total of 123 different RS variables were tested (Appendix A). Field-based models were used to inform variable selection for the RS-based models i.e. we made sure that we also tested RS variables that were similar to best variables selected into field-based models, and both modeling cases used the same training data of damaged and non-damaged plots from NFI. Subsequently, the RS- and field-based models were compared to assess differences in predictive performance and the influence of the independent variables.

We chose to use logistic regression as the final modeling approach, as this is a frequently used method in forest damage modeling (e.g., Valinger and Fridman, 1997, 2001; Saarinen et al., 2016; Suvanto et al.,

2021) and has been shown to provide comparable results to more complex non-parametric methods (e.g., Suvanto et al., 2019) such as generalized additive models (GAM, Hastie and Tibshirani, 1990) and boosted regression trees (Elith et al., 2008). Compared to non-parametric methods, logistic regression also benefits from more straightforward interpretation of the results, which is advantageous for future applications of the model.

After exploring the dataset and when the preliminary models for whole of Sweden performed less accurately, we decided to divide Sweden into two regions and create separate models for those (the North and the South region; Fig. 1). This was done to better account for the country's climatic and forest structural differences (Skogsstyrelsen, 2020), also observed in the data. In addition, as wind and snow damage are combined into one category in the Swedish NFI (wind/snow), dividing the country into two regions also helps to account for the difference in the primary damaging agents. In the South region, wind is the primary damage agent, whereas in the North, both wind and snow contribute more equally. The regions were defined based on the distribution of snow depth and load (mean of the maximum values) between 2007 and 2023 in Sweden (See 2.3 Weather data) and the borders of the sampling regions within the NFI, but also knowledge on differences in forest structure. Limits for dividing regions for the snow depth were circa 160 cm and snow load 0.95 kN/m^2. The number of plots was 15,066 in the North and 26,482 in the South for RS models and 15,341 and 26,358 for field-based models (Table 2), respectively, including 1.9% and 1.2% damaged plots. The number of plots used in NFI- and RS-based models differed slightly, which depended on RS/mapped data availability (missing pixels) or other detected errors in predictor variables in the modeling phase.

The following steps were employed for variable and model selection: First, a Simulated Annealing (SA) algorithm (Kirkpatrick et al., 1983) was used to identify the best-performing combinations of continuous variables (up to a maximum of 12) that explained vulnerability to wind and snow damage. Variables were first scaled and centered. GLM models ("MASS" v.7.3.65, Venables and Ripley, 2002; R Core Team, 2024) were applied to the North and the South regions. After obtaining the most suitable combinations of continuous predictors, the several variations of best fitting models were further refined, integrating available categorical variables. To do so, a stepwise regression ("MASS" v.7.3.65, Venables and Ripley, 2002; R Core Team, 2024) was applied to each candidate model to automatically identify the relevant categorical variables. Further, we supplemented automatic variable selection by manually introducing single candidate variables. During this phase, we often kept the variables with statistical and logical importance within the models and tested further attributes that we thought might improve model performance.

Categorical variables were excluded from the SA-procedure because their incorporation was not straightforward within this automated variable-selection framework. This was because the rare-event nature of the response (only 1.2–1.9% of plots are damaged): dummy expansion of multi-level factors frequently induced quasi-complete separation in the logistic GLM (Albert and Anderson, 1984) therefore isolating a handful of damaged individual indicator variables within the damaged plots. However, further we performed also a test combining categorical and

Table 2
Model results, including AUC values and explained deviation for RS- and field-based (NFI) models for the North and the South regions. Variables are descending order based on their importance in the model. * = Categorical variable, where the first class representing the reference class, is not listed in this table. See note in Table 1 for variable description.

Variables	Estimate	Std. error	Z value	Pr(>z)	AUC	Exp. Dev.
RS North					**0.77**	**0.11**
Intercept	−4.467	0.086	−51.86	< 0.001		
VolumeLodgepole	0.361	0.036	10.006	< 0.001		
zpcum6	−0.578	0.061	−9.486	< 0.001		
Snowdepth	0.603	0.065	9.240	< 0.001		
MaxWindWest	−0.537	0.094	−5.707	< 0.001		
Elevation	0.491	0.090	5.447	< 0.001		
Leaf-on data	0.205	0.055	3.740	< 0.001	*	
VolumeSpruce	0.156	0.060	2.580	0.009		
RS South					**0.69**	**0.04**
Intercept	−4.614	0.068	−67.469	< 0.001		
Pz_5.10	0.400	0.060	6.670	< 0.001		
Elevation1kmDiff	0.177	0.044	4.039	< 0.001		
VolumeSpruce	0.250	0.063	3.990	< 0.001		
zpcum4	−0.321	0.082	−3.891	< 0.001		
MaXWindNorth	0.175	0.052	3.378	< 0.001		
Diff_zq95_50m	0.201	0.063	3.198	0.001		
zq15	0.119	0.039	3.080	0.002		
zq30	−0.192	0.070	−2.758	0.006		
VolumePine	0.163	0.052	2.580	0.009		
VolumeLodgepole	0.085	0.034	2.543	0.011		
NFI					**0.80**	**0.16**
Intercept	−4.673	0.096	−48.527	< 0.001		
Mean height	0.846	0.083	10.242	< 0.001		
Prop. lodgepole	0.537	0.031	17.524	< 0.001		
Snowload	0.500	0.063	7.877	< 0.001		
MaxWindWest	−0.519	0.071	−7.302	< 0.001		
Time since thinning > 10 years	−0.157	0.044	−3.539	< 0.001	*	
Prop. deciduous/other	−0.248	0.089	−2.770	0.006		
NFI South					**0.73**	**0.07**
Intercept	−4.701	0.071	−65.884	< 0.001		
Height dif. closest stand	0.333	0.039	8.476	< 0.001		
Prop. lodgepole	0.139	0.024	5.775	< 0.001		
Time since thinning > 10 years	−0.264	0.046	−5.681	< 0.001	*	
MaxWindNorth	0.280	0.053	5.276	< 0.001		
Mean height	0.381	0.075	5.069	< 0.001		
Prop. spruce	0.251	0.058	4.364	< 0.001		
Elevation	0.191	0.052	3.659	< 0.001		

continuous variables. There the resulting problem of quasi-complete separation was overcome by merging rare and zero-event factor levels into an "Other" category and by fitting all candidate models with Firth's bias-reduced logistic regression (Firth, 1993) ("brglm2" v.1.1.0, Kosmidis and Firth, 2021; R Core Team, 2024). This did not lead to improvements in model performance, which retained us continuing with models from original variable selection.

Across all selection phases, multiple diagnostic metrics were applied to evaluate model performance. Variable selection was guided using the Akaike Information Criterion (AIC, "stats" 4.4.1, R Core Team, 2024) and the Area Under the Curve (AUC, "pROC" v.1.18.5, Robin et al., 2011; "caret" v.7.0.1, Kuhn, 2008; R Core Team, 2024): models with higher AUC and lower AIC were preferred, in order to limit overfitting (Akaike, 1981) and maintain an appropriate level of model complexity. Collinearity among the selected covariates was also assessed for every model using Pearson's correlation ("stats" v.4.4.1, R Core Team, 2024) and variance inflation factors (VIF, "car" 3.1.3, Fox and Weisberg, 2019; R Core Team, 2024). Variable pairs with correlation coefficients above 0.7 or a combination of variables showing a VIF value exceeding 3 (Zuur et al., 2010) were avoided in the final models. Furthermore, to evaluate how well the models captured variation in the response variables, we considered explained deviance, which quantifies the proportion of total deviance accounted for by the fitted model relative to a null model containing only an intercept (Ligges and Crawley, 2007). Higher explained deviance indicates better model fit and was used as an additional goodness-of-fit metric. Finally, the contribution of individual variables was assessed by examining their statistical significance ($p < 0.05$), variable importance ("caret" v7.0.1, Kuhn, 2008; R Core Team, 2024), and their logical coherence within the model.

The best candidate models were subsequently validated using a 10-fold cross-validation procedure with 10 repetitions, implemented via the 'repeatedCV' method ("caret" v7.0.1; Kuhn, 2008; R Core Team, 2024). This validation step allowed assessment of changes in variable significance and re-evaluation of all diagnostic metrics, including mean AUC, explained deviance, AIC, and VIF, while maintaining a constant proportion of damaged plots across folds. Through this process, we selected final best-fitting models for the two regions of interest (Table 2).

The application potential of the RS-based models was demonstrated by using the best-performing models to predict damage vulnerability across three study areas: two in the South and one in the North. Prior to prediction, each RS variable was collected from national maps or extracted from LiDAR data and resampled to a 30 × 30 m raster grid ("lidR" v.4.2.1, Roussel et al., 2020; "terra" v.1.8.17, Hijmans et al., 2025; R Core Team, 2024). Damage vulnerability maps were then generated by applying models over each study area, using RS metrics as spatial predictors (Fig. 7).

3. Results

The best RS model in the North region achieved an AUC value of 0.77 with 10-fold cross-validation, which was somewhat higher than that of the best RS model in the South region (AUC = 0.69). Both models included a combination of ALS point cloud metrics (zpcum6, zq15, zq30, Pz_5.10, zpcum4), terrain (Elevation, Elevation1kmDiff), tree species (VolumeSpruce, VolumePine, VolumeLodgepole) and weather information (Snowdepth, MaxWindWest, MaxWindNorth). The southern model had more ALS point cloud metrics and more tree species variables compared to the northern model, as well as information on the vegetation height difference within a 50 m radius (Diff_zq95_50m), whereas the northern model included "Snow depth" instead. All the best model candidates got very similar accuracies with just slightly different variable combination, i.e. the key elements in all best models were the same. This shows that similar results can be achieved using variant of similar metric as long it describes the same forest characteristics.

The best field-based models performed slightly better than the RS-based models and followed the same trend with better accuracy for the North compared to the South. The AUC value for the North was 0.80 and for the South 0.73. Variables such as "Mean tree height", "Proportion of lodgepole" and "Time since thinning" were included for both the northern and the southern field-based models. Separately, the best model for the North region included a "Proportion of deciduous species/other", "Snow load" and "Maximum wind from the west", while the best model for the South region accounted for "Proportion of lodgepole", "Height difference to neighboring stands", "Elevation" and "Maximum wind speed from the North direction". Surprisingly, the field-based model for the North did not include terrain information, while the RS-based model did. Time since thinning is the only variable that is not currently available as a country-wide dataset in Sweden.

Our results for all the models are presented in Table 2, where variables are ordered based on their influence, evaluated using the function VarImp() ("MASS" v.7.3.65, Venables and Ripley, 2002; R Core Team, 2024). The estimated coefficients shown in Table 2 are on the logit scale and therefore represent the log-odds of damage occurring given a one-unit change in the predictor, holding all other variables constant. In logistic regression, the model estimates the natural logarithm of the odds of the event (i.e., $\log[p/(1-p)]$), rather than the probability itself. However, positive log-odds coefficients indicate an increase in the probability of damage, whereas negative coefficient values indicate a decreasing probability of damage (Norton and Dowd, 2018). The density plots showing the distribution of predicted values for damaged and non-damaged plots are shown in Fig. 2.

The Marginal effects of key variables on damage probability are shown in Figs. 3–6, demonstrating the effects of different variables in the models. Damage probability rose with forest height in all four models, even if different metrics (ALS- or field-based) characterize this attribute in slightly different ways. In the RS-based northern model (Fig. 3), damage probability was governed by two opposing effects: it rose steeply with the lodgepole volume and declined steeply as the Zpcum6 increased, indicating lower damage where more returns originated low in the canopy. The elevation and the snow depth had moderate positive effects and the spruce volume a weak one. The maximum wind from the west showed a counterintuitive negative association with damage (interpreted in the Discussion). In the RS-based southern model (Fig. 4), the height percentile zq15 produced by far the steepest response, while the zq30 was essentially flat. Damage probability also increased markedly with the proportion of returns between 5 and 10 m (Pz_5.10) and with terrain ruggedness (Elevation1kmDiff) but declined as the Zpcum4 increased. The lodgepole volume had a moderate positive effect, and the spruce volume, the pine volume, the height difference within 50 m radius (Diff_zq95_50m) and the maximum wind from the north weaker positive ones.

In the field-based northern model (Fig. 5), damage probability increased steeply with the mean tree height, the proportion of lodgepole pine, and the snow load, which identified strong effect of the snow weight in the northern area during the wintertime. Stands that were thinned more than ten years ago were less likely to be damaged than recently thinned ones, and the proportion of deciduous/other species had a weak negative effect. Similarly to the RS northern model, the maximum wind from the west was negatively associated with damage. In the field-based southern model (Fig. 6), the proportion of lodgepole pine showed the strongest effect, followed by moderate positive effects of the height difference to the closest stand and the maximum wind from the north. The mean tree height, the proportion of spruce, and the elevation had weaker positive associations, and stands thinned more than ten years ago were again less susceptible than recently thinned ones.

To demonstrate the use of the models we created a damage vulnerability map for a test area using the northern model. In Fig. 7a-b, damage vulnerability is shown as a continuous range at the regional level, while Fig. 7c-d presents vulnerability classified into five classes at the local level.

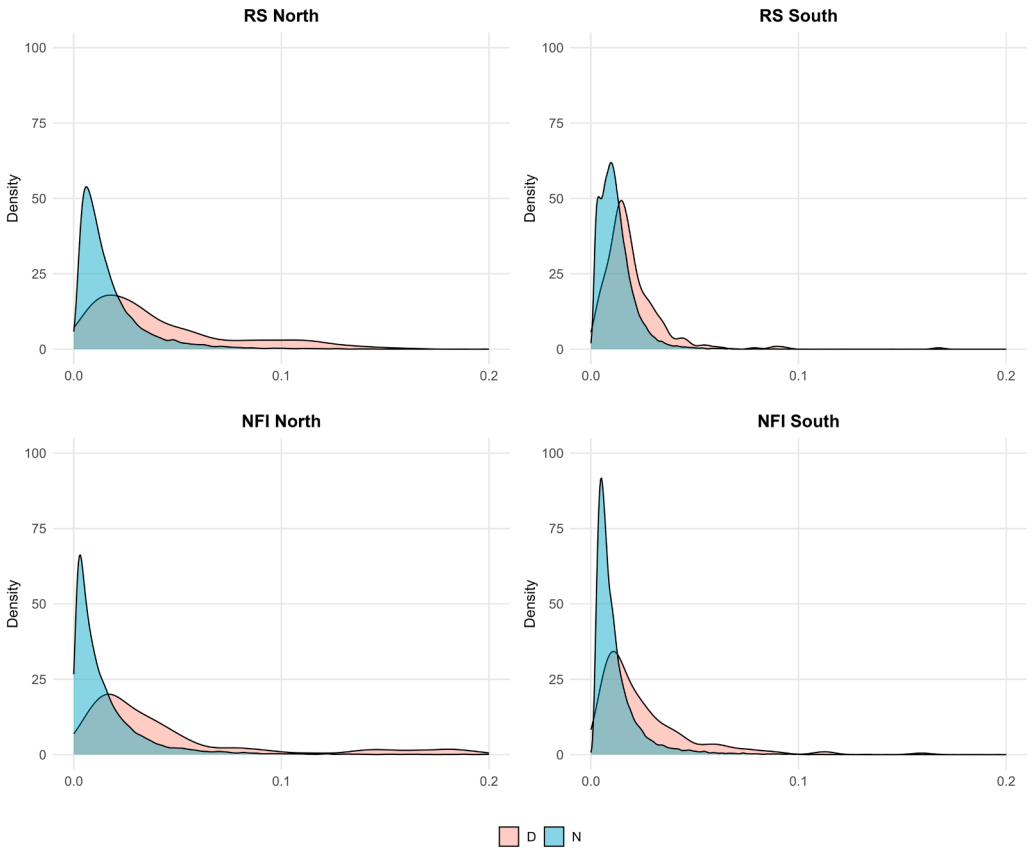

Fig. 2. Density distribution of the predicted damage probability of the damaged (D) and non-damaged (N) plots from RS-based and field-based (NFI) models in the North and the South regions.

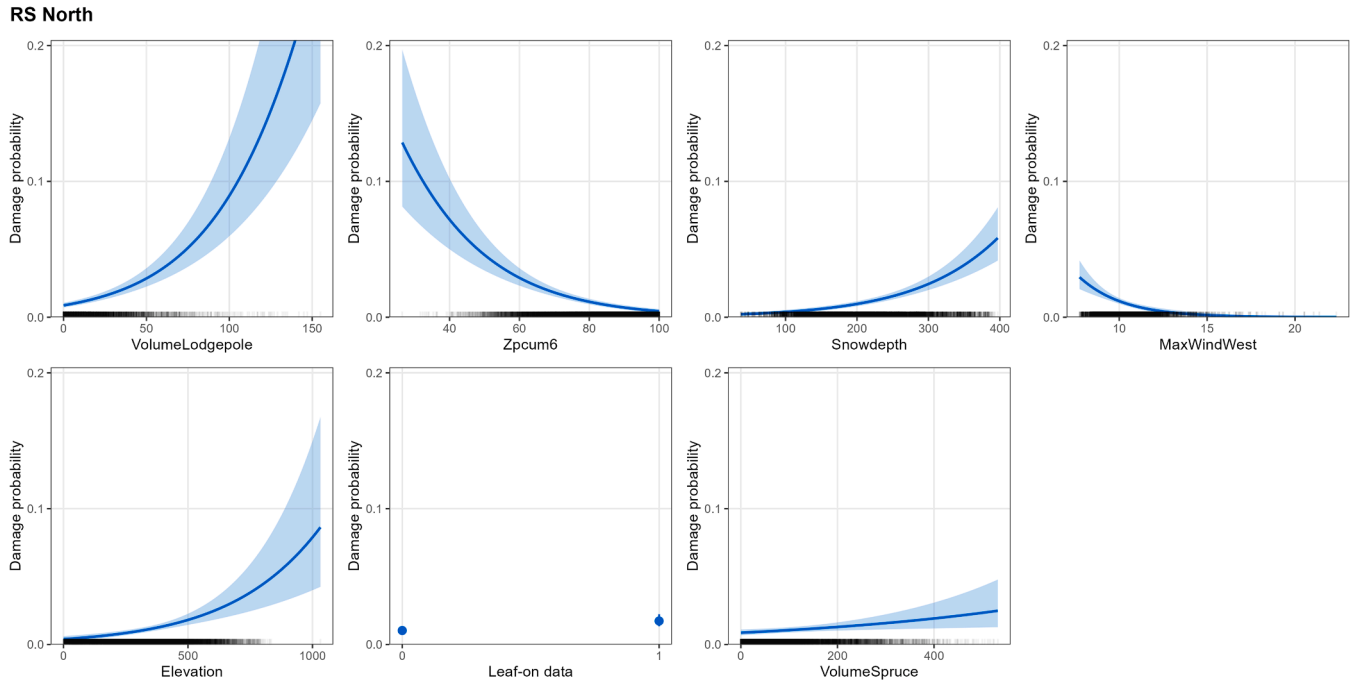

Fig. 3. Marginal effects of selected variables on damage probability for the RS-based model in the North region. Each panel shows the predicted damage probability as a function of one variable, while all other variables are held at their mean values (for continuous variables) or set to their reference category (for categorical variables). Solid lines represent the predicted mean, points indicate class-specific probabilities, and shaded areas or error bars denote the 95% prediction intervals. Rug plots along the x-axes illustrate the distribution of observed data.

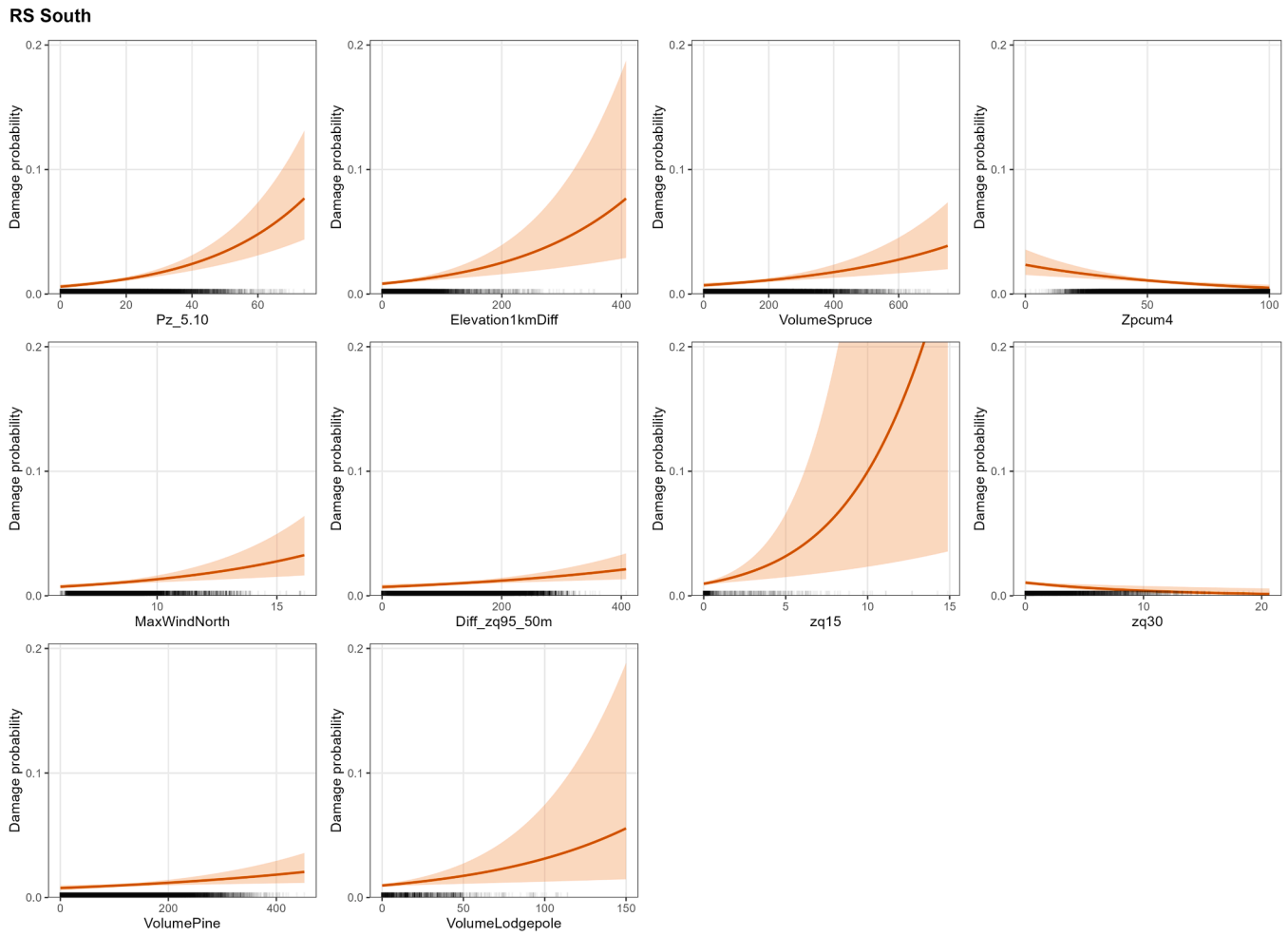

Fig. 4. Marginal effects of selected variables on damage probability for the RS-based model in the South region. Each panel shows the predicted damage probability as a function of one variable, while all other variables are held at their mean values (for continuous variables) or set to their reference category (for categorical variables). Solid lines represent the predicted mean, points indicate class-specific probabilities, and shaded areas or error bars denote the 95% prediction intervals. Rug plots along the x-axes illustrate the distribution of observed data.

4. Discussion

In this study we identified useful ALS metrics and combination of RS variables in modeling of wind and snow damage, compared the performance of ALS driven versus field-measured information in modeling damage vulnerability, and successfully created the first national vulnerability models for wind and snow damage based on a combination of ALS data, other mapped products, weather data and NFI data in Sweden. Unlike previous large-scale forest damage models, our approach used direct ALS metrics in the prediction models, allowing us to fully utilize the capacity of ALS to derive information about pre-damaged forest structure – a critical component in determining wind and snow damage vulnerability. This is because ALS point cloud contains more detailed information about the three-dimensional structure of the forest canopy compared to standard forest attributes (Lefsky et al., 1999; Maltamo et al., 2014). Earlier works on empirical forest wind and snow damage vulnerability models (e.g., Valinger and Fridman, 1997, 2011; Schmidt et al., 2010; Díaz-Yáñez et al., 2019) have largely used field-measured forest attributes. Whereas spatial vulnerability assessments "risk maps" have relied on already available maps of the forest variables included in the models (Suvanto et al., 2019, 2021; Merlin et al., 2025), not direct RS metrics.

The best RS-based vulnerability models included a combination of ALS-derived metrics, terrain height, dominant tree species information, and weather variables in both the northern and southern models. All selected variables were consistent with expectations and supported findings from earlier spatial studies (Suarez et al., 2008; Suvanto et al., 2019, 2021, Gopalakrishnan et al., 2020; Costa et al., 2023; Merlin et al., 2025). Direct ALS metrics used in the models included height percentiles "zq15" and "zq30" (15th and 30th percentiles of point heights) capturing vertical forest structure and stand slenderness, identified as primary vulnerability determinants (e.g., Peltola et al., 1999); the canopy density metrics "zpcum4" and "zpcum6" (cumulative percentage of returns located in the lower 40% or 60% of maximum elevation) capturing lower-canopy return density, a proxy for how exposed the sub-canopy is to wind loading (Russell et al., 2018); the interval metric "Pz_5.10" (proportion of returns between 5 and 10 m) also capturing information about density and vertical structure of the forest; finally "Diff_zq95_50m" (height difference inside a 50 m radius plot), which captures local height differentials to identify vulnerable forest edges where tall trees are exposed to wind damages (e.g., Gardiner, 2021). It is noteworthy that many candidate variables were excluded due to substantial overlap in the information they conveyed. As a result, variable retention was influenced, to some extent, by their redundancy rather than unique explanatory value (Dormann et al., 2013). Therefore, it is likely that alternative variable subsets could have been selected under slightly different conditions.

These ALS metrics represent complex features of the canopy structure which reflect not only tree height and stand density distribution (Maltamo et al., 2014) but also canopy and stand neighborhood

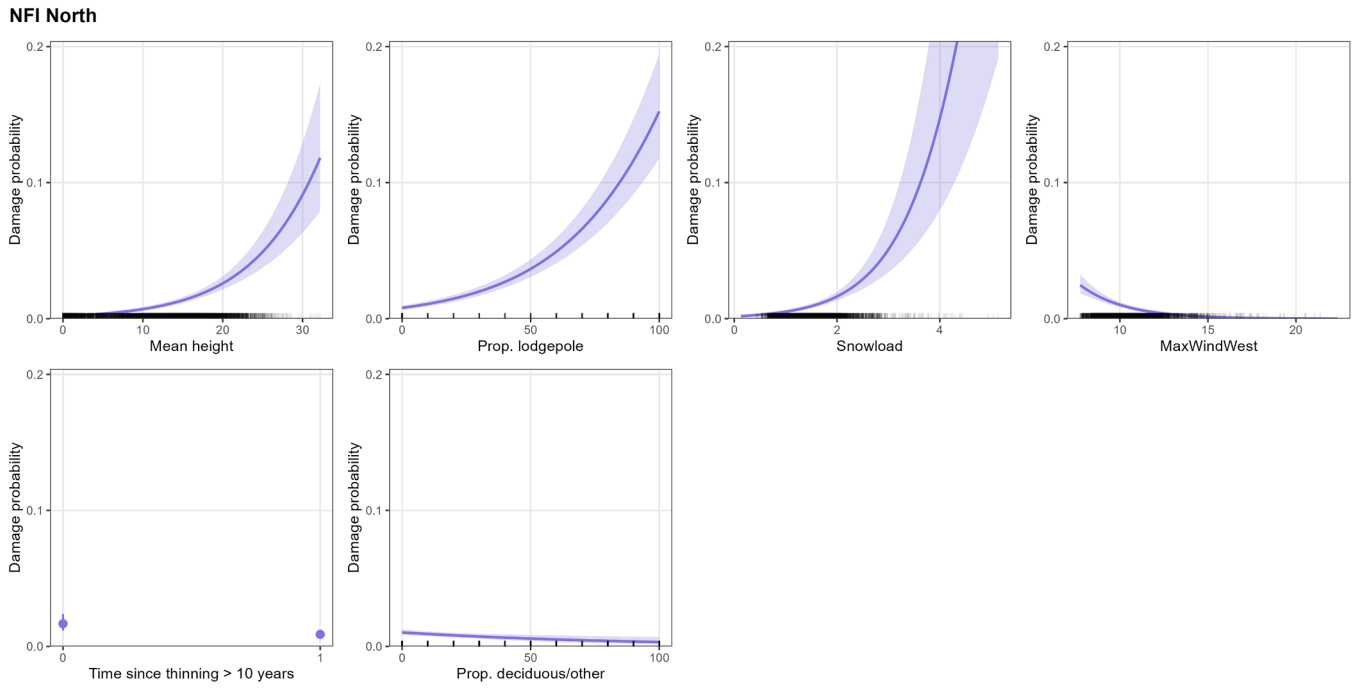

Fig. 5. Marginal effects of selected variables on damage probability for the field-based model in the North region. Each panel shows the predicted damage probability as a function of one variable, while all other variables are held at their mean values (for continuous variables) or set to their reference category (for categorical variables). Solid lines represent the predicted mean, points indicate class-specific probabilities, and shaded areas or error bars denote the 95% prediction intervals. Rug plots along the x-axes illustrate the distribution of observed data.

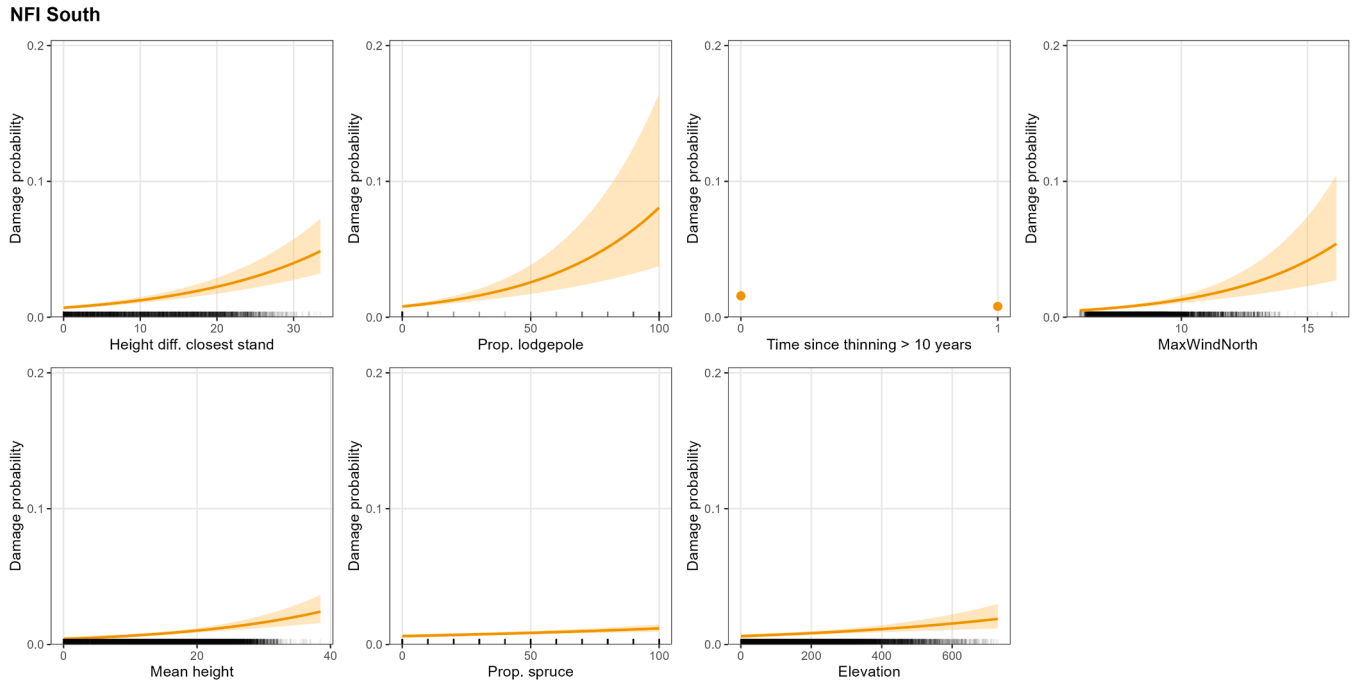

Fig. 6. Marginal effects of selected variables on damage probability for the field-based model in the South region. Each panel shows the predicted damage probability as a function of one variable, while all other variables are held at their mean values (for continuous variables) or set to their reference category (for categorical variables). Solid lines represent the predicted mean, points indicate class-specific probabilities, and shaded areas or error bars denote the 95% prediction intervals. Rug plots along the x-axes illustrate the distribution of observed data.

openness (e.g., Sasaki et al., 2008; Gopalakrishnan et al., 2020), and even tree species (crown structure), especially when combined with spectral data (e.g., Packalén and Maltamo, 2007; Ørka et al., 2009), which are key structural determinant of damage vulnerability based on previous findings (e.g., Nykänen et al., 1997; Peltola et al., 1999; Valinger and Fridman, 2011; Mitchell, 2013; Boudreault et al., 2014, Jackson et al., 2019; Suvanto et al., 2019; Gardiner, 2021). Therefore, they can serve as substitutes for mapped forest attribute data and have potential to bring more detailed information about the canopy and forest structure into the model, which are not necessarily captured by the

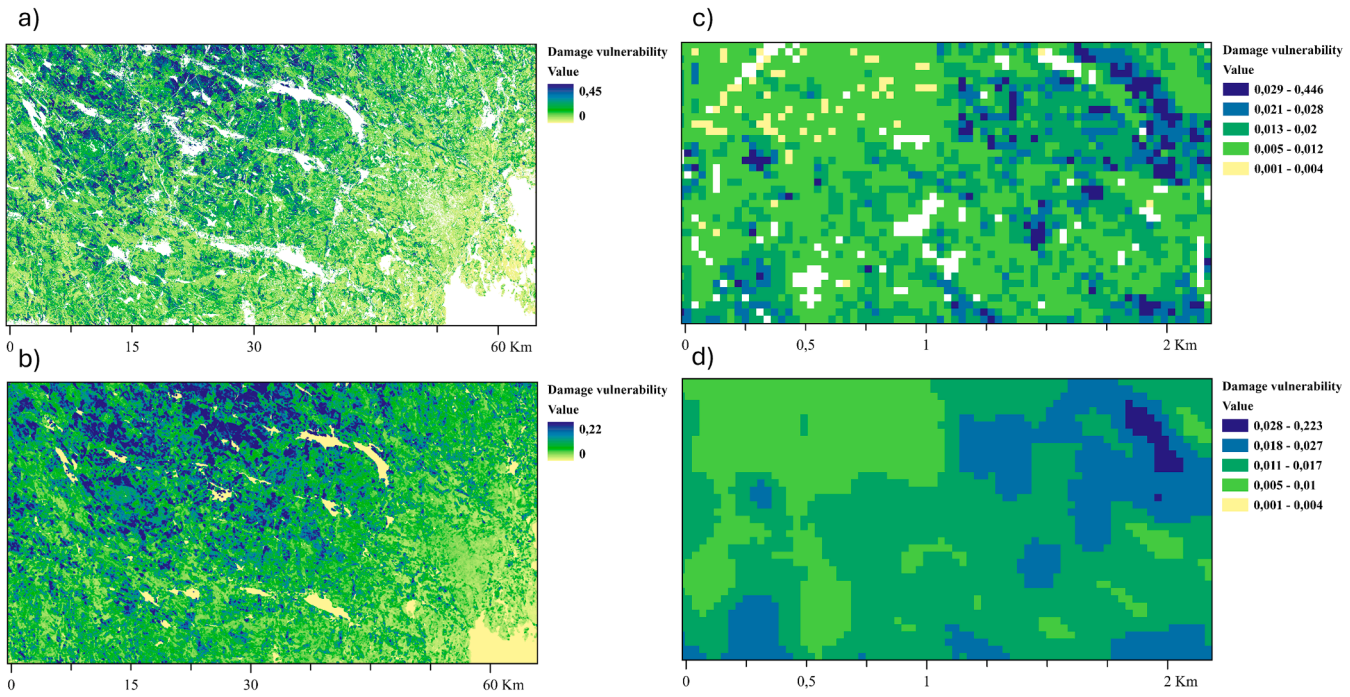

Fig. 7. Map demonstration for a case-study area in the North at the regional level using continuous scale (a-b) and at the local level using five vulnerability classes (c-d). Upper maps (a and c) are showing the original prediction map, while lower maps (b and d) are showing the smoothed version of maps to better indicate the hotspots of damage risk.

traditional field measurements.

In earlier studies, ALS data were first used to predict forest attributes, such as diameter at breast height, tree height, and stem density, based on the relationship between ALS metrics and field measurements (Suarez et al., 2008; Gopalakrishnan et al., 2020; Costa et al., 2023; Merlin et al., 2025), and later for forest vulnerability modeling. In addition, Saarinen et al. (2016) used ALS-based surface models (terrain and canopy height) when mapping the probability of wind-induced forest disturbances, and Gopalakrishnan et al. (2020) used ALS data to derive predictor variables, such as distance to edge and gap size, similarly to our height difference metrics. However, as said ALS data contains more information about forest structure, for example the detailed structure of the canopy and height differences, which are not described by variables such as tree height or gap size derived from ALS data in previous studies. Instead, by using a large range of direct ALS metrics, as we have done here, it is possible to more comprehensively utilize the potential of ALS data in identifying metrics that are linked to forest damage vulnerability.

As expected, the field-based vulnerability models had slightly better overall accuracies, likely due to the more accurate forest information from the field (direct measurement, forest attributes measured at same time with damage, spatial accuracy not being an issue etc. compared to RS data). Similar variables were selected for both field-based and RS-based models. However, the key difference was that field-derived structural variables were replaced with ALS-based metrics, which also included measures of height differences in the stand neighborhood. One important variable used in the field-based models was the "time since last thinning", which we could not include in the RS-based models since it is not currently available as an open wall-to-wall dataset in Sweden. The variables used in the field-based models have been included in several earlier studies (e.g., Nykänen et al., 1997; Peltola et al., 1999; Valinger and Fridman, 2011; Mitchell, 2013; Suvanto et al., 2019; Gardiner, 2021) and are therefore not discussed in detail here. It is worth mentioning the importance of the variable representing Lodgepole pine (*Pinus contorta*) due to its positive effect on damage vulnerability in both field- and RS-based models, a tree species that is seldom considered in forestry research in Fennoscandia. Earlier also Nicoll et al. (2006) found Lodgepole pine to be more susceptibility wind damage than other species when anchorage of different coniferous trees was studied. Lodgepole pine is a non-native species in Fennoscandia and is most commonly present in Sweden, where it covers around 1.6% of the growing stock (Skogsdata, 2025).

In this study, we divided Sweden into two modeling regions to take better account the large geographical variation in both climate and forest structure (Skogsstyrelsen, 2020). This was done after observing differences in the data and when preliminary models for whole Sweden performed less accurately. Variation in climate and forest conditions also affects the occurrence of different types of damage; for example, wind damage is most common in southern Sweden, while in northern Sweden both wind and snow damage occur frequently, often with combined effects, which was accounted using the regional models.

Both RS- and field-based vulnerability models showed higher modeling accuracy for the North region compared to the South region. Forest structure and tree species composition are more heterogeneous in southern Sweden, which may be one of the reasons. Similar results have been reported earlier by Valinger and Fridman (1997), where two counties in Sweden were compared. The Scandinavian Mountains also reach the northern part of southern Sweden, increasing variation in terrain and forest structure. Most of the predictors included in the models were similar in both regions, but differences were also identified. For example, snow variables were only included in the northern models, while height difference metrics in the stand neighborhood were only included in the southern models. In addition, the RS-based models for southern Sweden included more ALS-derived metrics and tree species variables i.e. more variables were needed to describe damage vulnerability indicating more complex system. Here, more research on combination of factors affecting damage processes across the region is needed. In the northern models (NFI and RS), maximum western wind speed (MaxWindWest) was unexpectedly negatively associated with damage probability. The variable was retained because it was not collinear with other predictors and contributed to model performance. This relationship should be interpreted cautiously. In snow-dominated northern

forests, stronger winds may reduce crown snow load by shedding intercepted snow and rime, thereby lowering the risk of snow-induced stem breakage (Nykänen et al., 1997; Lehtonen et al., 2014). In addition, long-term wind exposure may promote structural acclimation, increasing resistance to prevailing winds (Bonnesoeur et al., 2016). However, because observations were concentrated at low wind speeds, the negative effect may be weakly constrained at higher wind speeds and should not be overinterpreted.

4.1. Model limitations and further development

One challenge for our modeling approach was the combination of wind and snow damage in a single categorical variable within the Swedish NFI, while, for example, the Finnish NFI presents the two types of damage separately. This may impact on the results, as wind and snow can affect somewhat different types of forests in terms of forest structure and species composition. For example, previous research has shown that the probability of wind damage increases strongly with tree height and especially affects Norway spruce dominated forests (Suvanto et al., 2019), whereas snow damage typically impacts smaller trees, and Scots pine was found to be at higher risk (Nykänen et al., 1997; Suvanto et al., 2021; but see also Zubkov et al. 2024 who found more damage in Norway spruce compared to Scots pine in a study area in southern Norway). However, since wind and snow are part of same damage process (Peltola et al., 1999) the correct identification of wind and snow damage in the field can be challenging in regions where both damage types occur and can have a combined effect.

Another source of error in our models is the time difference between the laser scanning and the field inventory time point, which varies between 1–13 years. To account for differences in forest characteristics between the time of laser scanning and the time of damage, we removed plots that had been clearcut between the scanning and the field inventory, but forest growth during this time window was not considered. Furthermore, by using more advanced modeling methods, minor improvements in the models might have been achieved, even if earlier research did not find considerable improvements in model performance (Suvanto et al., 2019). We decided to use logistic regression due to its straightforward interpretation and its ease of use in future applications.

Creating a good model for damage probability is more challenging when the number of damaged plots is small. In this study, we included both temporary and permanent plots that had been inventoried in the field after the first and second national laser scanning of Sweden, but in the future more data will be available and can be used to improve the models, as the third scanning of Sweden started in 2025 (if the laser scanning data are not radically different between campaigns).

Finally, improvements in the nationally available datasets describing the predictor variables would improve the quality of the damage vulnerability maps. This is demonstrated in our results by the higher performance of models where the predictors are based on field measurements of the NFI plots, compared to RS-based models where the forest structure predictors are derived from national RS-based datasets. For example, improved change detection from satellite images would enable the mapping of forest thinnings (an important variable in field-based models) at the national level. In addition, development of improved forest information at the single-tree level, as well as improved soil type or tree species maps, may enable higher accuracy of damage probability maps in the future.

4.2. Application of the models

The application of these models to create wall-to-wall damage vulnerability maps can be a powerful tool for integrating risk information into forest management decisions. However, the models focus on damage from smaller-scale events and do not account for the most extreme storms. By visualizing vulnerability across the landscape, the maps reveal regional and stand-level variation in risk, supporting decisions on the timing and intensity of final felling or thinning in vulnerable areas. For practical use, they could be complemented by uncertainty maps showing prediction errors (Wadoux and Heuvelink, 2023). Ultimately, the implications of vulnerability information depend on each forest owner's risk tolerance and management objectives. Therefore, rather than defining a universal threshold for 'high--risk' or 'low-risk' stands, risk classifications should remain context-specific and adaptable (Fig. 7).

The maps also have applications beyond forest management. Snow- or wind-damaged trees can cause substantial harm to infrastructure, including power lines, roads, and buildings. In Finland, forest snow damage probability maps (Suvanto et al., 2021) have proven useful for identifying sections of power line networks at risk from snow-damaged trees (Räisänen et al., 2023). They can also support the rapid identification of forests requiring salvage logging after major disturbance events. For example, Laapas et al. (2023) showed that combining the Finnish wind damage probability map (Suvanto et al., 2019) with storm impact data effectively mapped likely storm-damaged areas. Such information supports authorities in coordinating damage management and helps forest owners identify when on-site inspections are needed, particularly when they live far from their properties.

Damage probability models can also be integrated with forest simulation models to assess how management strategies influence forest sensitivity to damage over time (e.g., Potterf et al., 2022; Öhman et al., 2025). These simulations commonly rely on field-based models, including the NFI-based model developed in this study. Our improved field-based vulnerability model could be implemented in the Heureka decision support system (Lämås et al., 2023), replacing or complementing its current wind damage risk model (Lagergren et al., 2012). In the future, RS-based models may also be incorporated into next-generation of Heureka, enabling more detailed spatial planning of forest landscapes.

5. Conclusions

In this study, we successfully demonstrated how vulnerability to wind and snow damage can be predicted using a combination of ALS, weather and other mapped data and NFI field measurements in Sweden. In contrast to earlier large-scale forest damage models, we used direct ALS metrics in the prediction models, allowing us to fully utilize the capacity of ALS to derive information on complex features of forest structure reflecting tree height, slenderness, stand density, canopy and stand neighborhood openness, and tree species, which are the key structural determinant of damage vulnerability. Both RS- and field-based models combined forest structural variables (ALS- or field-based), tree species, terrain, and weather information, showing that damage vulnerability is governed by multiple interacting biophysical factors. We observed clear regional differences in model performance and selected variables between North and South regions, highlighting spatial variation in underlying damage processes. Overall, we provide a practical approach for mapping forest damage risk from local to national levels, supporting both operational forest management and strategic planning. These models represent a first step towards national-wide damage vulnerability maps for Sweden, planned for production during 2026.

CRediT authorship contribution statement

Inka Bohlin: Writing – review & editing, Writing – original draft, Visualization, Validation, Supervision, Project administration, Methodology, Investigation, Funding acquisition, Conceptualization. **Victor Manabe:** Writing – review & editing, Visualization, Validation, Software, Methodology, Investigation, Formal analysis, Data curation. **Emanuele Papucci:** Writing – review & editing, Writing – original draft, Visualization, Validation, Software, Methodology, Investigation, Formal analysis, Data curation. **Olivia Fors:** Writing – review & editing,

Visualization, Validation, Software, Methodology, Investigation, Formal analysis, Data curation. **Sven Adler:** Writing – review & editing, Validation, Supervision, Software, Methodology, Investigation. **Susanne Suvanto:** Writing – review & editing, Writing – original draft, Validation, Methodology, Investigation, Funding acquisition, Conceptualization. **Bertil Westerlund:** Writing – review & editing, Resources, Data curation.

Funding

This study has got financing from Skogssällskapet in project "Mapping risk for wind and snow damage with state-of-art remote sensing" (2023–1117-Steg 2 2022 LIABE), SLU Forest damage center, Vinnova (2023–02783), SLU Environmental monitoring and analysis program Climate, Natural Resource Institute Finland, and Swedish Forest Agency, and Open access funding by Swedish University of Agricultural Sciences (SLU).

Declaration of Competing Interest

The authors declare the following financial interests/personal relationships which may be considered as potential competing interests: Inka Bohlin reports financial support was provided by Skogssällskapet. Inka Bohlin reports financial support was provided by Vinnova. Inka Bohlin reports financial support was provided by Swedish Forest Agency. If there are other authors, they declare that they have no known competing financial interests or personal relationships that could have appeared to influence the work reported in this paper.

Acknowledgments

We thank Swedish Forest Agency for the good collaboration during the project.

Appendix A. Supporting information

Supplementary data associated with this article can be found in the online version at doi:10.1016/j.foreco.2026.124040.

Data availability

Data will be made available on request.

References

Ågren, A., Lindgren, W., 2020. Dokumentation nya hydrografiska kartor – vattendrag och SLU Markfuktighetskartor. Swedish University of Agricultural Sciences. (Swedish) ⟨https://www.slu.se/globalassets/slu.se/om-slu/organisation/institutioner/sesko/peatmaps/dokumentation-slu-markfuktighetskarta-2020-11-12.pdf⟩.

Akaike, H., 1981. Likelihood of a model and information criteria. J. Econom. 16 (1), 3–14. https://doi.org/10.1016/0304-4076(81)90071-3.

Albert, A., Anderson, J.A., 1984. On the existence of maximum likelihood estimates in logistic regression models. Biometrika 71 (1), 1–10. https://doi.org/10.1093/biomet/71.1.1.

Asada, R., Hurmekoski, E., Hoeben, A.D., Patacca, M., Stern, T., Toppinen, A., 2023. Resilient forest-based value chains? Econometric analysis of roundwood prices in five European countries in the era of natural disturbances. For. Policy Econ. 153, 102975. https://doi.org/10.1016/j.forpol.2023.102975.

Bonnesoeur, V., Constant, T., Moulia, B., Fournier, M., 2016. Forest trees filter chronic wind-signals to acclimate to high winds. New. Phytol. 210, 850–860. https://doi.org/10.1111/nph.13836.

Boudreault, L.-É., Bechmann, A., Sørensen, N.N., Sogachev, A., Dellwik, E., 2014. Canopy structure effects on the wind at a complex forested site. J. Phys. Conf. Ser. 524, 012112. https://doi.org/10.1088/1742-6596/524/1/012112.

Costa, M., Gardiner, B., Locatelli, T., Marchi, L., Marchi, N., Lingua, E., 2023. Evaluating wind damage vulnerability in the Alps: a new wind risk model parametrisation. Agric. For. Meteorol. 341, 109660. https://doi.org/10.1016/j.agrformet.2023.109660.

Díaz-Yáñez, O., Mola-Yudego, B., González-Olabarria, J.R., 2019. Modelling damage occurrence by snow and wind in forest ecosystems. Ecol. Model. 408, 108741. https://doi.org/10.1016/j.ecolmodel.2019.108741.

Dormann, C.F., Elith, J., Bacher, S., Buchmann, C., Carl, G., Carré, G., Marquéz, J.R.G., Gruber, B., Lafourcade, B., Leitão, P.J., Münkemüller, T., McClean, C., Osborne, P.E., Reineking, B., Schröder, B., Skidmore, A.K., Zurell, D., Lautenbach, S., 2013. Collinearity: a review of methods to deal with it and a simulation study evaluating their performance. Ecography 36, 27–46. https://doi.org/10.1111/j.1600-0587.2012.07348.x.

Elith, J., Leathwick, J.R., Hastie, T., 2008. A working guide to boosted regression trees. J. Anim. Ecol. 77, 802–813. https://doi.org/10.1111/j.1365-2656.2008.01390.x.

Firth, D., 1993. Bias reduction of maximum likelihood estimates. Biometrika 80 (1), 27–38. https://doi.org/10.1093/biomet/80.1.27.

Fox, J., Weisberg, S., 2019. An R Companion to Applied Regression, 3rd ed. Sage Publications, Thousand Oaks, CA ⟨https://www.john-fox.ca/Companion/⟩.

Fridman, J., Holm, S., Nilsson, M., Nilsson, P., Ringvall, A.H., Ståhl, G., 2014. Adapting National Forest Inventories to changing requirements – the case of the Swedish National Forest Inventory at the turn of the 20th century. Silva Fenn. 48 (3), 1095. https://doi.org/10.14214/sf.1095.

Gardiner, B., 2021. Wind damage to forests and trees: a review with an emphasis on planted and managed forests. J. For. Res. 26 (4), 248–266. https://doi.org/10.1080/13416979.2021.1940665.

Gardiner, B., Byrne, K., Hale, S., Kamimura, K., Mitchell, S.J., Peltola, H., Ruel, J.C., 2008. A review of mechanistic modelling of wind damage risk to forests. For 81 (3), 447–463. https://doi.org/10.1093/forestry/cpn022.

Gardiner, B., Lorenz, R., Hanewinkel, M., Schmitz, B., Bott, F., Szymczak, S., Frick, A., Ulbrich, U., 2024. Predicting the risk of tree fall onto railway lines. For. Ecol. Manag. 553, 121614. https://doi.org/10.1016/j.foreco.2023.121614.

Gopalakrishnan, R., Packalen, P., Ikonen, V.P., Räty, J., Venäläinen, A., Laapas, M., Pirinen, P., Peltola, H., 2020. The utility of fused airborne laser scanning and multispectral data for improved wind damage risk assessment over a managed forest landscape in Finland. Ann. For. Sci. 77, 97. https://doi.org/10.1007/s13595-020-00992-8.

Groenemeijer, P., Becker, N., Djidara, M., Gavin, K., Hellenberg, T., Holzer, A.M., Juga, I., Jokinen, P., Jyhä, K., Lehtonen, I., Mäkelä, H., Napoles, O.M., Nissen, K., Paprotny, D., Prak, P., Púčik, T., Tijssen, L., Vajda, A., 2015. Past cases of extreme weather impact on critical infrastructure in Europe. Deliverable D2.2, RAIN Project. ⟨http://rain-project.eu/wp-content/uploads/2015/11/D2.2-Past-Cases-final.compressed.pdf⟩.

Hart, E., Sim, K., Kamimura, K., Meredieu, C., Guyon, D., Gardiner, B., 2019. Use of machine learning techniques to model wind damage to forests. Agric. For. Meteorol. 265, 16–29. https://doi.org/10.1016/j.agrformet.2018.10.022.

Hastie, T.J., Tibshirani, R.J., 1990. Generalized additive models. In: Monographs on Statistics and Applied Probability, 43. Chapman and Hall, New York, p. 352.

Hijmans, R.J., Barbosa, M., Bivand, R., Brown, A., Chirico, M., Cordano, E., Dyba, K., Pebesma, E., Rowlingson, B., Sumner, M.D., 2025. terra: spatial data analysis. R. Package Version 1, 8–70. https://doi.org/10.32614/CRAN.package.terra.

Jackson, T., Shenkin, A., Kalyan, B., Zionts, J., Calders, K., Origo, N., Disney, M., Burt, A., Raumonen, P., Malhi, Y., 2019. A new architectural perspective on wind damage in a natural forest. Front. For. Glob. Change 1. https://doi.org/10.3389/ffgc.2018.00013.

Kirkpatrick, S., Gelatt, C.D., Vecchi, M.P., 1983. Optimization by simulated annealing. Science 220, 671–680. https://doi.org/10.1126/science.220.4598.671.

Komonen, A., Schroeder, L.M., Weslien, J., 2011. Ips typographus population development after a severe storm in a nature reserve in southern Sweden. J. Appl. Entomol. 135, 132–141. https://doi.org/10.1111/j.1439-0418.2010.01520.x.

Korhonen, K.T., Ahola, A., Heikkinen, J., Henttonen, H.M., Hotanen, J.P., Ihalainen, A., Melin, M., Pitkänen, J., Räty, M., Sirviö, M., Strandström, M., 2021. Forests of Finland 2014–2018 and their development 1921–2018. Silva Fenn. 55 (5), 10662. https://doi.org/10.14214/sf.10662.

Kosmidis, I., Firth, D., 2021. Jeffreys-prior penalty, finiteness and shrinkage in binomial-response generalized linear models. Biometrika 108 (1), 71–82. https://doi.org/10.1093/biomet/asaa052.

Kuhn, M., 2008. Building predictive models in R using the caret package. J. Stat. Softw. 28 (5), 1–26. https://doi.org/10.18637/jss.v028.i05.

Laapas, M., Suvanto, S., Peltoniemi, M., Venäläinen, A., 2023. Combining interpolated maximum wind gust speed and forest vulnerability for rapid post-storm mapping of potential forest damage areas in Finland. For 96 (5), 690–704. https://doi.org/10.1093/forestry/cpad005.

Lagergren, F., Jönsson, A.M., Blennow, K., Smith, B., 2012. Implementing storm damage in a dynamic vegetation model for regional applications in Sweden. Ecol. Modell. 247, 71–82. https://doi.org/10.1016/j.ecolmodel.2012.08.011.

Lämås, T., Sängstuvall, L., Öhman, K., Lundström, J., Årevall, J., Holmström, H., Nilsson, L., Nordström, E.-M., Wikberg, P.-E., Wikström, P., Eggers, J., 2023. The multi-faceted Swedish Heureka forest decision support system. Context, functionality, design, and 10 years experiences of its use. Front. For. Glob. Change 6, 1163105. https://doi.org/10.3389/ffgc.2023.1163105.

Lantmäteriet, 2022. Laser data Download, NH. Lantmäteriet. ⟨https://www.lantmateriet.se/globalassets/geodata/geodataprodukter/hojddata/e_pb_laserdata_nedladdning_nh.pdf⟩.

Lantmäteriet, 2024. Laser data Download, forest. Lantmäteriet. ⟨https://www.lantmateriet.se/globalassets/geodata/geodataprodukter/hojddata/e_pb_laserdata_nedladdning_skog.pdf⟩.

Lefsky, M.A., Cohen, W.B., Acker, S.A., Parker, G.G., Spies, T.A., Harding, D., 1999. Lidar remote sensing of the canopy structure and biophysical properties of Douglas-Fir Western Hemlock forests. Remote. Sens. Environ. 70, 339. ⟨https://andrewsforest.oregonstate.edu/sites/default/files/lter/pubs/pdf/pub3488.pdf⟩, 36.

Lehtonen, I., Hoppula, P., Pirinen, P., Gregow, H., 2014. Modelling crown snow loads in Finland: a comparison of two methods. Silva Fenn. 48 (3), 1120. https://doi.org/10.14214/sf.1120.
Lehtonen, I., Kämäräinen, M., Gregow, H., Venäläinen, A., Peltola, H., 2016. Heavy snow loads in Finnish forests respond regionally asymmetrically to projected climate change. Nat. Hazards Earth Syst. Sci. 16 (10), 2259–2271. https://doi.org/10.5194/nhess-16-2259-2016.
Ligges, U., Crawley, M.J., 2007. The R Book. Stat. Pap. 50, 445–446. https://doi.org/10.1007/s00362-008-0118-3.
Maltamo, M., Næsset, E., Vauhkonen, J., 2014. Forestry applications of airborne laser scanning, concept and case studies. Managing Forest Ecosystems, vol 27. Springer, Dordrecht. 464 p. https://doi.org/10.1007/978-94-017-8663-8.
Merlin, M., Locatelli, T., Gardiner, B., Astrup, R., 2025. Large-scale modelling wind damage vulnerability through combination of high-resolution forest resources maps and ForestGALES. For. Ecosyst. 14, 100361. https://doi.org/10.1016/j.fecs.2025.100361.
Mitchell, S.J., 2013. Wind as a natural disturbance agent in forests: a synthesis. For 86 (2), 147–157. https://doi.org/10.1093/forestry/cps058.
National Forest Inventory, 2022. Fältinstruktion 2022. Dept. of Forest Resource Management, Swedish University of Agricultural Sciences, Umeå. (Swedish) ⟨https://www.slu.se/globalassets/slu.se/om-slu/organisation/institutioner/skoglig-resurshushallning/riksskogstaxeringen/dokument/faltinstruktioner/22_ris_fin.pdf⟩.
Naturvårdsverket, 2023. Nationella marktäckedata 2018, basskikt. Produktbeskrivning. Naturvårdsverket. (Swedish) ⟨https://geodata.naturvardsverket.se/nedladdning/marktacke/NMD2018/NMD_Produktbeskrivning_NMD2018Basskikt.pdf⟩.
Nicoll, B.C., Gardiner, B.A., Rayner, B., Peace, A.J., 2006. Anchorage of coniferous trees in relation to species, soil type, and rooting depth. Can. J. For. Res. 36, 1871–1883. https://doi.org/10.1139/x06-072.
Nilsson, M., Nordkvist, K., Jonzén, J., Lindgren, N., Axensten, P., Wallerman, J., Egberth, M., Larsson, S., Nilsson, L., Eriksson, J., Olsson, H., 2017. A nationwide forest attribute map of Sweden predicted using airborne laser scanning data and field data from the National Forest Inventory. Remote. Sens. Environ. 194, 447–454. https://doi.org/10.1016/j.rse.2016.10.022.
Norton, E.C., Dowd, B.E., 2018. Log Odds and the Interpretation of logit models. Health Serv. Res. 53, 859–878. https://doi.org/10.1111/1475-6773.12712.
Nykänen, M.-L., Broadgate, M., Kellomäki, S., Peltola, H., Quine, C., 1997. Factors affecting snow damage of trees with particular reference to European conditions. Silva Fenn. 31 (2), 5618. https://doi.org/10.14214/sf.a8519.
Öhman, K., Llorente, I.P., Fustel, T., Bohlin, I., Lämås, T., Eggers, J., 2025. Integrating wind damage vulnerability into long-term forest planning: an optimisation-based model for spatial decision support. Trees For. People 20, 100870. https://doi.org/10.1016/j.tfp.2025.100870.
Ørka, H.O., Næsset, E., Bollandsås, O.M., 2009. Classifying species of individual trees by intensity and structure features derived from airborne laser scanner data. Remote. Sens. Environ. 113 (6), 1163–1174. https://doi.org/10.1016/j.rse.2009.02.002.
Packalén, P., Maltamo, M., 2007. The k-MSN method for the prediction of species-specific stand attributes using airborne laser scanning and aerial photographs. Remote. Sens. Environ. 109 (3), 328–341. https://doi.org/10.1016/j.rse.2007.01.005.
Pawlik, Ł., Harrison, S.P., 2022. Modelling and prediction of wind damage in forest ecosystems of the Sudety Mountains, SW Poland. Sci. Total. Environ. 815, 151972. https://doi.org/10.1016/j.scitotenv.2021.151972.
Peltola, H., Kellomäki, S., Väisänen, H., Ikonen, V.-P., 1999. A mechanistic model for assessing the risk of wind and snow damage to single trees and stands of Scots pine, Norway spruce, and birch. Can. J. For. Res. 29 (6), 647–661. https://doi.org/10.1139/x99-029.
Potterf, M., Eyvindson, K., Blattert, C., Burgas, D., Burner, R., Jörg, G.S., Mönkkönen, M., 2022. Interpreting wind damage risk – how multifunctional forest management impacts standing timber at risk of wind felling. Eur. J. For. Res. 141, 347–361. https://doi.org/10.1007/s10342-022-01442-y.
R Core Team, 2024. R: a language and environment for statistical computing. R Foundation for Statistical Computing, Vienna, Austria. ⟨https://www.R-project.org/⟩ (Accessed 3.6.2026).
Räisänen, O., Suvanto, S., Haapaniemi, J., Lassila, J., 2023. Crown snow load outage risk model for overhead lines. Appl. Energy 343, 121183. https://doi.org/10.1016/j.apenergy.2023.121183.
Robin, X., Turck, N., Hainard, A., Tiberti, N., Lisacek, F., Sanchez, J.-C., Müller, M., 2011. pROC: an open-source package for R and S+ to analyze and compare ROC curves. BMC Bioinform. 12, 77. https://doi.org/10.1186/1471-2105-12-77.
Roussel, J.-R., Auty, D., Coops, N.C., Tompalski, P., Goodbody, T.R.H., Meador, A.S., Bourdon, J.-F., Boissieu, F., Achim, A., 2020. lidR: an R package for analysis of airborne laser scanning (ALS) data. Remote. Sens. Environ. 251, 112061. https://doi.org/10.1016/j.rse.2020.112061.
Roussel, J.-R., Goodbody, T.R.H., Tompalski, P., 2025. The lidR package. ⟨https://r-lidar.github.io/lidRbook/⟩ (Accessed 7.10.2025).
Russell, E.S., Liu, H., Thistle, H., Strom, B., Greer, M., Lamb, B., 2018. Effects of thinning a forest stand on sub-canopy turbulence. Agric. For. Meteorol. 248, 295–305. https://doi.org/10.1016/j.agrformet.2017.10.019.
Saarinen, N., Vastaranta, M., Honkavaara, E., Wulder, M.A., White, J.C., Litkey, P., Holopainen, M., Hyyppä, J., 2016. Using multi-source data to map and model the predisposition of forests to wind disturbance. Scand. J. For. Res. 31 (1), 66–79. https://doi.org/10.1080/02827581.2015.1056751.
Sasaki, T., Imanishi, J., Ioki, K., Morimoto, Y., Kitada, K., 2008. Estimation of leaf area index and canopy openness in broad-leaved forest using an airborne laser scanner in comparison with high-resolution near-infrared digital photography. Landsc. Ecol. Eng. 4, 47–55. https://doi.org/10.1007/s11355-008-0041-8.
Schmidt, M., Hanewinkel, M., Kändler, G., Kublin, E., Kohnle, U., 2010. An inventory-based approach for modeling single-tree storm damage — experiences with the winter storm of 1999 in southwestern Germany. Can. J. For. Res. 40 (8), 1636–1652. https://doi.org/10.1139/X10-099.
SGU, 2025a. Jordarter 1:25 000 – 1:100 000. Sveriges Geologiska undersökning. Produktbeskrivning. (Swedish) ⟨https://resource.sgu.se/dokument/produkter/jordarter-25-100000-beskrivning.pdf⟩.
SGU, 2025b. Jorddjupsmodell. Sveriges Geologiska undersökning. Produktbeskrivning. (Swedish) ⟨https://resource.sgu.se/dokument/produkter/jorddjupsmodell-beskrivning.pdf⟩.
Skogsdata, 2007. Dept. of Forest Resource Management, Swedish University of Agricultural Sciences, Umeå. (Swedish) ⟨https://pub.epsilon.slu.se/3403/1/Skogsdata2007.pdf⟩.
Skogsdata, 2025. Dept. of Forest Resource Management, Swedish University of Agricultural Sciences, Umeå. (Swedish) ⟨https://www.slu.se/globalassets/slu.se/om-slu/organisation/institutioner/skoglig-resurshushallning/riksskogstaxeringen/dokument/skogsdata/skogsdata_2025_web.pdf⟩.
Skogsstyrelsen, 2020. Forest management in Sweden - Current practice and historical background. Report 2020/4. ⟨https://www.skogsstyrelsen.se/globalassets/om-oss/rapporter/rapporter-20222021202020192018/rapport-2020-4-forest-management-in-sweden.pdf⟩.
Skogsstyrelsen, 2024. Utförda avverkningar – produktbeskrivning. Skogstyrelssen. (Swedish) ⟨https://www.skogsstyrelsen.se/globalassets/sjalvservice/karttjanster/geodatatjanster/produktbeskrivningar/utforda-avverkningar---produktbeskrivning.pdf⟩.
SLU, 2018. SLU Skogskarta - Trädslag. Dept. of Forest Resource Management, Swedish University of Agricultural Sciences. Produktbeskrivning. (Swedish).
SMHI, 2023. Daily mean values from observation data of temperature, wind speed and wind direction, snow depth and snow load between 2007-2023 from Sweden. Swedish Meteorological and Hydrological Institute, December 2023 [Ordered dataset].
SMHI, 2025. Stormar i Sverige. Swedish Meteorological and Hydrological Institute. (Swedish) ⟨https://www.smhi.se/kunskapsbanken/meteorologi/stormar-i-sverige/20240222/norden⟩ (Accessed 3.6.2026).
Suarez, J., Garcia, R., Gardiner, B., Patenaude, G., 2008. The estimation of wind risk in forest stands using airborne laser scanning (ALS) (<special issue> silvilaser). J. For. Plan. 13, 165–185. https://doi.org/10.20659/jfp.13.special_issue_165.
Suvanto, S., Lehtonen, A., Nevalainen, S., Lehtonen, I., Viiri, H., Strandström, M., Peltoniemi, M., 2021. Mapping the probability of forest snow disturbances in Finland. PLoS. ONE 16 (7), e0254876. https://doi.org/10.1371/journal.pone.0254876.
Suvanto, S., Peltoniemi, M., Tuominen, S., Strandström, M., Lehtonen, A., 2019. High-resolution mapping of forest vulnerability to wind for disturbance-aware forestry. For. Ecol. Manag. 453, 117619. https://doi.org/10.1016/j.foreco.2019.117619.
Tompalski, P., Goodbody, T.R.H., 2025. LidRmetrics. ⟨https://github.com/ptompalski/lidRmetrics⟩ (Accessed 3.6.2026).
Torresani, M., Montagnani, L., Rocchini, D., Moudrý, V., Andreoli, A., Wellstein, C., Koyanagi, K., Da Ros, L., Bacaro, G., Perrone, M., Salvatori, C., Menegaldo, I., Guatelli, E., Tognetti, R., 2024. LiDAR insights on stand structure and topography in mountain forest wind extreme events: The Vaia case study. Agric. For. Meteorol. 359, 110267. https://doi.org/10.1016/j.agrformet.2024.110267.
Valinger, E., Fridman, J., 1997. Modelling probability of snow and wind damage in Scots pine stands using tree characteristics. For. Ecol. Manag. 97 (3), 215–222. https://doi.org/10.1016/S0378-1127(97)00062-5.
Valinger, E., Fridman, J., 2011. Factors affecting the probability of windthrow at stand level as a result of Gudrun winter storm in southern Sweden. For. Ecol. Manag. 262 (3), 398–403. https://doi.org/10.1016/j.foreco.2011.04.004.
Venables, W.N., Ripley, B.D., 2002. Modern Applied Statistics with S, 4th ed. Springer, New York. https://doi.org/10.1007/978-0-387-21706-2.
Wadoux, A.-C., Heuvelink, G.B.M., 2023. Uncertainty of spatial averages and totals of natural resource maps. Methods Ecol. Evol. 14, 1320–1332. https://doi.org/10.1111/2041-210X.14106.
Wallentin, C., Nilsson, U., 2014. Storm and snow damage in a Norway spruce thinning experiment in southern Sweden. For 87 (2), 229–238. https://doi.org/10.1093/forestry/cpt046.
Zubkov, P., Gardiner, B., Nygaard, B.E., Guttu, S., Solberg, S., Eid, T., 2024. Predicting snow damage in conifer forests using a mechanistic snow damage model and high-resolution snow accumulation data. Scand. J. For. Res. 39 (1), 59–75. https://doi.org/10.1080/02827581.2023.2289660.
Zuur, A.F., Ieno, E.N., Elphick, C.S., 2010. A protocol for data exploration to avoid common statistical problems. Methods Ecol. Evol. 1, 3–14. https://doi.org/10.1111/j.2041-210X.2009.00001.x.